1985

Stress computations for hybrid composites /

Chwang-Liang Yang
Lehigh University

STRESS COMPUTATIONS FOR HYBRID COMPOSITES

by

Chwang-Liang Yang

A Thesis

Presented to the Graduate Committee

of Lehigh University

in Candidacy for the Degree of

Master of Science

in

Mechanical Engineering and Mechanics

Lehigh University

1984

ACKNOWLEDGMENTS

I would like to express my sincerely thanks to my advisors, Professor T. J. Delph and Professor D. G. Harlow for their patient guidance, direction, and encouragement. Under their truthful direction, I was able to complete my master program successfully.

I would like to give most thanks to my dear parents, parents-in-law, and my dearest wife for their endless encouragement and warm blessings.

I would like to express my appreciation to Mrs. Joan Decker for helping me type this thesis.

CERTIFICATE OF APPROVAL

This thesis is accepted and approved in partial fulfillment of the requirements for the degree of Master of Science in Mechanical Engineering and Mechanics.

December 3, 1984
(Date)

D G Harlow
Professor in Charge

F. Erdogan
Chairman of the Department

Table of Contents

1. Abstract

The stress redistribution in a hybrid composite sheet due to fiber fractures has been studied. The shear-lag model was used to perform the analysis. The hybrid composite is modeled as a single layer tape containing both high modulus and low modulus fibers in a common matrix. Stress concentration factors for surviving fibers and ineffective lengths for broken fibers have been computed for various configurations of broken and unbroken fibers. The shear-lag analysis was used with a Monte Carlo simulation to model the hybrid composite strength.

2. Introduction

Recently, there has been increasing interest in the use of hybrid composites which consist of two or more types of reinforcing fibers in a common matrix. This is partly because conventional engineering materials have been replaced in some weight-critical applications by composite materials using filaments such as glass, carbon, boron or an aramid such as Kevlar 49 in a matrix material. Hybrid composites offer a range of properties that cannot be obtained from composite materials with a single kind of reinforcing fiber. For instance, adding carbon fibers to a glass fiber composite substantially increases the ultimate stress or strain of a laminate. At the same time, material costs and manufacturing costs can be substantially reduced by blending some cheaper fibers with more expensive ones. For instance, if we mix about 20% by volume of graphite fibers with glass fibers, we can produce a composite with about 75% of the strength and stiffness properties of an all graphite reinforced laminate, but the cost is only 30% of the all graphite material. Other examples of the applications and mechanical properties of hybrid composites can be found in survey papers such as references [1-8].

If the potential applications of hybrid composites are to be realized, the failure mechanism under different load histories must be understood and characterized. As with many composites, the

tensile behavior of hybrid composites is not fully understood. One important reason for the inability to accurately describe tensile failure is attributed to the 'hybrid effect'. Marom et al. [9] defined the 'hybrid effect' as a positive or negative deviation of a centain mechanical property from the rule-of-mixtures behavior. The more common definition for the 'hybrid effect' is the observed increase in failure strain of the hybrid composite with respect to composites consisting of the constituent having the lowest ultimate strain. There are many publications which discuss the existence of the 'hybrid effect'. Hayashi [10] is credited as the first person who observed this 'hybrid effect'. Bunsel and Harris [11] later observed the 'hybrid effect' in their tests on unidirectional laminates made from separate layers of graphite and glass fibers. Their conclusion is that the 'hybrid effect' cannot be attributed to the residual compressive thermal strains in the graphite. Chamis et al. [12] tested four different hybrid systems, each of them consisting of three different volume ratios of the constituent fibers. They conclude that hybrid composites are stronger than composites consisting of the weaker constituent. Another series of experiments was conducted by Zweben [13], who observed the 'hybrid effect' in hybrid composites made by combining 'Kevlar' 49 and 'Thornel' 300 graphite fibers in a Fiberite 934 epoxy matrix. Zweben also concluded that residual thermal strains alone cannot explain the 'hybrid effect'. Thus, we can conclude that the 'hybrid effect'

does exist even if the effect is small. It is apparent that the 'hybrid effect' must be quantified more accurately in order for hybrid composites to be readily usable.

The mechanical basis for the hybrid effect remains somewhat puzzling. We know that when one or more fibers is suddenly broken under applied load in a composite, the load in the broken fiber or fibers must be transferred through the common matrix to the adjacent fibers in order to restore equilibrium. Hence, we would like to characterize the stress redistribution in the surviving, adjacent fibers so that we can more precisely predict gross mechanical properties such as failure stress, failure strain and the hybrid effect. In this work, the stress concentration factors resulting from the presence of one or more broken fibers are calculated for the surviving adjacent fibers in hybrid composites with fibers arranged unidirectionally in single layers with various configurations and volume ratios.

Hedgepeth [14] was the first person to describe the stress redistribution around a broken fiber in a unidirectionally reinforced sheet. He derived the stress concentration factor for surviving fibers adjacent to an array of broken fibers by using a simple shear-lag theory. Zweben [15] calculated the strain concentration factor at the tip of a notch in a unidirectional hybird composite by applying a similar approximate method. Fukuda

and Kawata [16] derived the stress concentration factor in a composite laminate consisting of several discontinuous layers. They concluded that the concentration factor obtained by Hedgepeth could be obtained from their analysis by increasing the number of layers. Fukuda and Chou [17] considered the stress concentration factors for hybrid composites with high modulus fibers and low modulus fibers alternated. They introduced the concept of influence functions as proposed by Hedgepeth to derive the stress concentration factor. They concluded that for a hybrid composites containing both high modulus and low modulus fibers, the stress concentration factor on high modulus fibers adjacent to a crack is lower than that in an all-high modulus fiber composite for the same number of fractured fibers. One omission in their work is that they did not compute the stress concentration factors for surviving fibers between two cracks. The stress concentration factors for surviving fibers between two cracks is always greater than that for fibers adjacent to a single crack.

The ineffective length δ_1 is also of interest. This quantity is a measure of the axial dimension over which the stress is perturbed in the vicinity of a broken fiber in an unidirectional composite. For a composite with only one type of fiber, the ineffective length is easy to define, but for hybrid composites, the situation is somewhat more complicated. Based upon a shear-lag analysis, it should depend upon the number of each type of broken

fibers, the mechanical properties of the fibers and matrix, the size of the composites, and the geometry of the specimen.

The purpose of this work is to carry out calculations for stress concentration factors and ineffective lengths in unidirectional hybrid composites for various configurations and volume ratios of broken fibers and to utilize these results in a statistical failure model. This model is intended to estimate the tensile failure of hybrid composites and to predict the effect of various volume ratios and degrees of constituent fiber dispersion upon the failure behavior.

3. Mathematical analysis

Our primary purpose is to provide some insight into the failure strength of a composite material containing two types of fibers with different stiffness characteristics. To do this, we adopt the shear-lag analysis of Zweben [15]. We consider the hybrid composite to be modeled by a single layered tape containing n continuous unidirectional fibers of length l. Each fiber is either a low or a high modulus fiber. A typical representation of a planar tape with a volume ratio of 1:1 and fully dispersed fibers is shown in Figure 1.

We denote the high modulus fibers as HM with subscript 1, and the low modulus fibers as LM with subscript 2. The respective moduli and cross-sectional area of the fibers are denoted by E_1, A_1 and E_2, A_2. We assume that the unidirectional fibrous composite is subjected to a tensile force in the fiber direction. We will assume that the fibers are linearly elastic until fracture, and that the effective fiber area is equal to the total cross-sectional area of the fibers in the bundle. We denote the axial load and displacement of the i^{th} fiber as $P_i(x)$ and $U_i(x)$, and x=0 indicates the plane of fiber fracture. Let us consider the equilibrium of the single fiber shown in Figure 2. We can write down the equation expressing equilibrium in the fiber direction as:

$$P_i + (dP_i/dx)dx - P_i - (\tau_1+\tau_2)hdx = 0 \qquad (1)$$

where τ is the shear stress carried by the matrix, h is the thickness of the sheet, x is the axial coordinate along the fiber.

By Hooke's Law and the linearized strain-displacement relation:

$$\varepsilon_i = dU_i/dx$$

$$\sigma_i = E \quad \varepsilon = E(dU_i/dx)$$

$$P_i = A\sigma_i = EA(dU_i/dx)$$

$$dP_i/dx = EA(d^2U_i/dx^2)$$

where ε_i is the axial strain in the i^{th} fiber and σ_i is the axial stress in the i^{th} fiber. Then, the equilibrium equation (1) becomes:

$$EA(d^2U_i/dx^2) - (\tau_1 + \tau_2)h = 0 \qquad (2)$$

The shear stress τ is carried by the matrix. Let us consider the situation shown in Figure 3. We compute the shear stresses τ_1, τ_2 by

$$\gamma_1 = (U_i - U_{i-1})/d$$

$$\gamma_2 = (U_i - U_{i+1})/d$$

$$\tau_1 = G\gamma_1 = G(U_i - U_{i-1})/d$$

$$\tau_2 = G\gamma_2 = G(U_i - U_{i+1})/d$$

where γ_1, γ_2 are the shear strains existing in the matrix and G denotes the shear modulus of the matrix. We substitute the expressions for τ_1, τ_2 into equation (2), and the equilibrium equation for the i^{th} fiber then becomes finally

$$EA(d^2U_i/dx^2) + Gh(U_{i-1}+U_{i+1}-2U_i)/d = 0 \qquad (3)$$

If the j^{th} fiber is a high modulus fiber and the k^{th} fiber is a low modulus fiber, we can write the respective equilibrium equations as :

$$E_1A_1(d^2U_j/dx^2) + Gh(U_{j-1}+U_{j+1}-2U_j)/d = 0 \qquad (4)$$

$$E_2A_2(d^2U_k/dx^2) + Gh(U_{k-1}+U_{k+1}-2U_k)/d = 0 \qquad (5)$$

It is assumed that axial stresses in the matrix are negligible, and the matrix serves as a medium for transmission of shear stress alone. For convenience, we would like to express the equilibrium equation in a non-dimensional form. To do this, we must change the displacements U_i into dimensionless displacements u_i, and the axial coordinate x into a dimensionless axial coordinate ξ. These dimensionless variables are related to the corresponding dimensional variables by :

$$U_i = \varepsilon u_i[E_2A_2d/Gh]^{1/2} \quad , \quad i=1,2,3, \ \cdots$$

$$x = \xi[E_2A_2d/Gh]^{1/2}$$

where ε is the value of the uniform axial strain as x goes to ∞. We introduce another dimensionless parameter R_a, the ratio of the

extensional stiffness of fibers as

$$R_\alpha = E_\alpha A_\alpha / E_2 A_2 \quad , \quad \alpha = 1,2$$

so that, $R_1 = E_1 A_1 / E_2 A_2$, $R_2 = 1$. The use of these nondimensional parameters yields the equilibrium equations in dimensionless form as:

$$R_{\alpha i}(d^2 U_i / d\xi^2) + U_{i-1} + U_{i+1} - 2U_i = 0 \tag{6}$$

We now assume that the tape represents a portion of a larger body in which the axial strain has the constant value ε. Let us denote the displacement in the fibers adjacent to the boundaries of the tape as U_1, U_n. The equilibrium equation for these fibers will be:

$$E_{\alpha 1} A_{\alpha 1}(d^2 U_1 / dx^2) + Gh(U_2 - 2U_1)/d = -Gh\varepsilon x/d \tag{7}$$

$$E_{\alpha n} A_{\alpha n}(d^2 U_n / dx^2) + Gh(U_{n-1} - 2U_n)/d = -Gh\varepsilon x/d \tag{8}$$

or in dimensionless form as :

$$R_{\alpha 1}(d^2 u_1 / d\xi^2) + u_2 - 2u_1 = -\xi \tag{9}$$

$$R_{\alpha n}(d^2 u_n / d\xi^2) + u_{n-1} - 2u_n = -\xi \tag{10}$$

We can now write down the governing set of linear differential equations for the system of n fibers as :

$$\begin{cases} R_{a1}(d^2u_1/d\xi^2) + u_2 - 2u_1 = -\xi \\ R_{a2}(d^2u_2/d\xi^2) + u_1 + u_3 - 2u_2 = 0 \\ R_{a3}(d^2u_3/d\xi^2) + u_2 + u_4 - 2u_3 = 0 \\ - - - - - - - - - - - - - \\ R_{an}(d^2u_n/d\xi^2) + u_{n-1} - 2u_n = -\xi \end{cases} \tag{11}$$

we can express equation (11) in operational form as :

$$\begin{bmatrix} D^2 - 2/R_{a1} & 1/R_{a1} & 0 - - - - - - - - 0 \\ 1/R_{a2} & D^2 - 2/R_{a2} & 1/R_{a2} & 0 & - - - 0 \\ - - - - - - - - - - - - - - - - - - - \\ - - - - - - - - - - & 1/R_{an} & D^2 - 2/R_{an} \end{bmatrix} \begin{Bmatrix} u_1 \\ u_2 \\ - \\ u_n \end{Bmatrix} = \begin{Bmatrix} -\xi/R_{a1} \\ 0 \\ - \\ -\xi/R_{an} \end{Bmatrix} \tag{12}$$

where D is the linear operator :

$$D = d/dx \quad \text{and} \quad D^2 = d^2/dx^2$$

In order to solve the system of equation (12), we look for homogeneous solutions of the form as :

$$u_i^H = A_i e^{r\xi}, \quad i=1, 2, 3, \cdots n, \tag{13}$$

Thus,

$$\begin{bmatrix} r^2-2/R_{\alpha 1} & 1/R_{\alpha 1} & 0 & \cdots & 0 \\ 1/R_{\alpha 2} & r^2-2/R_{\alpha 2} & 1/R_{\alpha 2} & \cdots & 0 \\ \cdots & \cdots & \cdots & \cdots & \cdots \\ \cdots & \cdots & 1/R_{\alpha n} & r^2-2/R_{\alpha n} & \end{bmatrix} \begin{Bmatrix} A_1 u_1 \\ A_2 u_2 \\ - \\ A_n u_n \end{Bmatrix} = \begin{Bmatrix} 0 \\ 0 \\ - \\ 0 \end{Bmatrix} \tag{14}$$

A non-singular solution of equation (14) exists if and only if the determinant of the coefficient matrix is zero. Hence r is obtained as the solution of

$$\begin{vmatrix} r^2-2/R_{\alpha 1} & 1/R_{\alpha 1} & 0 & \cdots & 0 \\ 1/R_{\alpha 2} & r^2-2/R_{\alpha 2} & 1/R_{\alpha 1} & \cdots & 0 \\ 0 & \cdots & \cdots & \cdots & 0 \\ 0 & \cdots & 0 & 1/R_{\alpha n} & r^2-2/R_{\alpha n} \end{vmatrix} = 0 \tag{15}$$

It is apparent that obtaining values of r which satisfy equation (15) is equivalent to solving an eigenvalue problem. In order that the displacement components be bounded, the value of r must be negative. Then, the homogeneous solution may be written as :

$$u_i = \sum_{j=1}^{n} A_{ij} e^{r_j \xi} \tag{16}$$

where A_{ij} is the eigenvector corresponding to the eigenvalue r_j. It can readily be seen that the particular solutions to equations (12) are given by

$$u_i^p = \xi \tag{17}$$

Thus the general solution becomes

$$u_i = \xi + \sum_{j=1}^{n} A_{ij} e^{r_j \xi} \tag{18}$$

At the origin, we note that the stress in the broken fibers is zero and the displacement in the unbroken fibers is zero. Therefore, the boundary conditions at $\xi=0$ will be $du_i(0)/d\xi = 0$ for broken fibers and $u_j(0) = 0$ for unbroken fibers.

The strain concentration factor associated with an unbroken fiber is defined as the ratio of the strain at x=0 to the uniform strain ε is

$$K_i = (1/\varepsilon)(dU_i(0)/dx) \tag{19}$$

or in dimensionless form :

$$K_i = du_i(0)/d\xi \tag{20}$$

From equation (18) and (20), we can find the strain concentration factors for the unbroken fibers by :

$$K_i = 1 + \sum_{j=1}^{n} A_{ij} r_j \tag{21}$$

Because we assume that all fibers are linearly elastic until fracture, the strain concentration factor and the stress concentration factor are identical.

Now, let us consider the ineffective length δ_i. We make use of the definition proposed by Friedman [18], where the strain distribution in the broken fiber is replaced by a step function that has the same average strain. Figure 4 shows the concept schematically. Thus we require that the areas between the actual and the equivalent step function strain distribution curves and the constant strain ε be equal. Suppose that the i^{th} fiber is broken, Then we have

$$\delta_i \varepsilon/2 = \int_0^\infty (\varepsilon - dU_i/dx)dx \tag{22}$$

or in dimensionless form :

$$\delta_i = 2[E_1 A_1 d/R_{ai} Gh]^{1/2} \int_0^\infty (1 - du/d\xi)d\xi \tag{23}$$

from equation (18), we can obtain :

$$du_i/d\xi = 1 - \sum_{j=1}^{n} A_{ij} r_j e^{-r_j \xi} \tag{24}$$

From equation (23), we can now compute the ineffective length for a broken fiber as :

$$\begin{aligned} \delta_i &= 2[E_1 A_1 d/R_{ai} Gh]^{1/2} \left(\sum_{j=1}^{n} A_{ij} e^{-r_j \xi} \right) \Big|_{\xi=0}^{\xi=\infty} \\ &= 2[E_1 A_1 d/R_{ai} Gh]^{1/2} \left(\sum_{j=1}^{n} A_{ij} \right) \end{aligned} \tag{25}$$

4. Numerical results

We consider a hybrid composite model with 15 fibers arranged in the form of a single layered tape. The hybrid composite is assumed to contain two kinds of fibers, that is high modulus fibers and low modulus fibers. The fibers are arranged with high modulus fibers and low modulus fiber alternated and the two boundary fibers are high modulus fibers. A schematic is shown in Figure 5.

From the analysis of the previous section, the stress concentration factor for a surviving fiber adjacent to a broken fiber depends upon the quantity $R_1 = E_1A_1/E_2A_2$. Calculations will be presented for the values R_1=1,2,3. When R_1 equals 1 with one fiber broken, the stress concentration factor of the surviving fibers directly adjacent to the broken fiber is calculated to be 1.331. By way of comparison, Hedgepeth [14] obtained a value of 1.333, Zweben [15] a value of 1.293, and Fukuda and Chou [17] a value of 1.342. The model of Hedgepeth and Zweben just contained a very few unbroken fibers and only one broken fiber. However, Fukuda and Chou made their calculation for more than fifteen broken fibers. They conducted the calculation by using the concept of influence functions proposed by Hedgepeht [14], and they expressed the solutions in the form of Fourier series. Hence, slight differences may be expected between their results and those presented here. The numerical techniques used in the present work, in which the stress

concentration factors depend upon the results of an eigenvalue problem, is felt to be more flexible and slightly more accurate then that used by Fukuda and Chou, because of errors involved in the truncation of the Fourier Series. The comparison between the result made by the present techniques and those due to Fukuda and Chou is shown in Table 1.

It should be noted that Fukuda and Chou calculated the stress concentration factor for the surviving fiber directly adjacent to a crack. A crack is taken to mean a group of adjacent broken fibers. They did not compute the stress concentration factor on a surviving fiber located between two cracks. This situation, however, often arises in statistical simulations, and hence will be considered in the present work. It was found that the stress concentration factor for a surviving fiber located between two cracks is greater than that for a surviving fiber directly adjacent to a crack with an equal number of broken fibers.

When a fiber is broken, the stress will be redistributed to surviving fibers in order to maintain mechanical equilibrium, that is, every surviving fiber will have an increase in stress produced by each broken fiber. Hence every surviving fiber will have a concentration factor greater than one even if the value is not much greater than one. Tables 2-4 show the concentration factors of every surviving fiber associated with different configurations of broken

fibers for different values of the extensional stiffness ratio R. The symbol '*' represents a broken fiber.

The ineffective length produced by broken fibers in different situations is shown in Tables 6-9. If we let $[E_1A_1/Gh]^{1/2}$ be a constant, then according to our calculations, the values shown in the tables are $2[d/R_{ai}]^{1/2}(\sum_{j=1}^{n}A_{ij})$. We note that the ineffective length of a broken fiber is a function of extensional stiffness, distance between two fibers, thickness, and shear modulus of matrix.

5. Statistical analysis

Basic probability distribution functions: Let $G_n(e)$ be the c.d.f.(cumulative distribution function) for the breaking strain of a single bundle with n fiber segments. This c.d.f. depends upon the c.d.f. for the breaking strain of the fiber segments $F_v(e,\delta)$, v=H,L, and it depends upon the strain concentration factors K_i calculated by the shear lag analysis. Furthermore, $G_n(e)$ is dependent upon the geometrical dispersion, i.e. the arrangement of the fibers and the volume ratio of the fibers. Thus, $G_n(e)$ is quite difficult to compute, nevertheless, it is the main c.d.f. which must be evaluated.

Let $H_{m,n}(e)$ be the c.d.f. for the breaking strain of the hybrid. Because the hybrid is conceptualized as a series of statistically independent and identically distributed bundles, the weakest link formulation of extreme value theory is applicable. Thus :

$$H_{m,n}(e)=1-[1-G_n(e)]^m,\ e\geq 0 \tag{26}$$

It is clearly manifest why $G_n(e)$ is such an important c.d.f. The statistical behavior of the hybrid can be understood only if $G_n(e)$ is accurately estimated. This is the focus of the numerical simulation described in the next section.

Monte Carlo simulation: In order to investigate the effect of volume ratio and dispersion on ultimate strain and ultimate strength, the Monte Carlo simulation method is employed. Simulation is a statistical type approach which has its greatest benefit in that analytical complexities are circumvented. Conceptually the hybrid model is rather simple, and consequently simulation is straightforward. Nevertheless, many geometrically complicated hybrid problems can be studied with quite good success.

The simulations were conducted for a single bundle so that $G_n(\epsilon)$ could be estimated. The number of fibers in the bundle was assumed to be 90. For each specific choice of volume ratio and dispersion considered, 25 replicate simulations were conducted. Since the breaking strain ε_i^v, v=H,L, were assumed to be the fundamental random variables, simulated values for ε_i^v were generated based upon the Weibull c.d.f.:

$$F_v(\epsilon,\delta)=1-\exp[-(\epsilon/\varepsilon_\delta^v)^{\rho_v}], \quad \epsilon\geq 0, \quad v=H,L. \tag{27}$$

where ρ_v is the shape parameter, and ε_δ^v is the scale parameter.

According to the results of Harlow [19], Fukuda and Chow [24], the simulations for the hybrids should follow a Weibull c.d.f. very closely which is also commonly observed from experimentation. Thus, the Monte Carlo simulations are reasonably accurate, and they are representative for small laboratory specimens so that comparisions

to experimental data is justified.

Material parameters: In order to perform a simulation which is meaningful, representative material parameters must be chosen. One of the hybrid systems which has been studied is a mixture of carbon and Kevlar 49 in a common matrix [13]. Phoenix and Wu [20] carefully measured many of the parameters for Kevlar 49. They reported an elastic modulus of 131 GPa and a fiber diameter of 11.89 μm. For a 5 cm long Kevlar 49, the estimated Weibull shape parameter is ρ=8.2 which corresponds to approximately 14% coefficient of variation. They also estimated the Weibull scale parameter for strength to be 3590 MPa which corresponds to 2.7% strain, assuming linear elastic conditions. Manders and Bader [21] reported that high tensile strength carbon fibers have a Weibull shape parameter of approximately ρ=7.0 which corresponds to about 16% coefficient of variation. The estimated scale parameter for strength for 5 cm specimens is 1720 MPa or 0.72% strain. Earlier [22] they reported an elastic modulus of 240 GPa. Typically the carbon fiber diameter is between 7 and 9 μm. The values reported by Zweben [13] are consistent with these. Thus, several simulations are based upon the following parameter values: E_{II}=240 GPa, ρ_{II}=7.0, ε_0^{II}=0.0072, E_L=131 GPa, ρ_L=8.2, and ε_0^{L}=0.027.

Simulation results: If we introduce these concentration factors computed by the shear-lag analysis in a Monte Carlo

simulation, it will enable us to describe the fracture of hybrid composites more accurately. For the statistical simulation we generated a group of random numbers taken to be the breaking strains of every single fiber. The first break occurs in the weakest fiber and the stress is redistributed on surviving fibers because of the force equilibrium. Every time when we sweep breaking strains of surviving fibers we can obtain a next weakest breaking strain. Using this method, we can find a clusters of broken fibers. When all fibers are broken then the greatest value of these weakest breaking strains is the breaking strain of the hybrid.

Three different volume ratio of hybrid composites were considered here. They are 1:0, 1:1, 2:1 of H-fibers to L-fibers. In each case the simulated results were plotted on Weibull probability paper. Figures 6, 7 and 8 are typical examples based upon the carbon/Kevlar hybrid parameters given above, where e is the breaking strains of hybrid composites, and P is Weibull c.d.f. as shown in the figure. Figure 6 is for the case of a volume ratio of 2:1 of H-fibers to L-fibers with maximum dispersion, i.e., the geometrical pattern is a cluster of two H-fibers and one L-fiber repeated a total of 30 times to account for the total number of 90 fibers. The notation of 2H:1L is used to designate this description and similarly for other patterns. Figure 7 is for a scheme of H-fibers and L-fiber alternated, and Figure 8 is for a scheme of all H-fibers. It is manifest that a Weibull c.d.f. fits the data quite

well. The estimated Weibull c.d.f. was obtained by finding the linear least squares fit to the data as plotted on Weibull paper. The probability plotting positions ${}_nP_i$ were assumed to be the mean value of the fraction of the sampled values occurring before the i^{th} ordered observation, i.e., ${}_nP_i=i/(n+1)$ or specifically ${}_{25}P_i=i/26$. Also included on the graphs are the 95% and 5% rank confidence bands. The two-sided 90% confidence band indicates that the Weibull c.d.f. is an appropriate choice for the c.d.f. of the simulated data. Note that near the median the bands are close implying a sharp estimate, but in the upper and lower tails where the data is more sparse, the bands are wider so that the estimate is not as good. As a final comment, the slope of the line serves as an estimator for the Weibull shape parameter of the hybrid, and the Weibull scale parameter is most easily estimated by the inverse Weibull function evaluated at a probability of 63.2%. Both estimators are easy to find from the Weibull graph, e.g., on Figure 6 the shape and scale parameters ρ_c and ε_c for the hybrid are 24.7 and 0.521%, respectively, and correspondingly for Figure 7, ρ_c=28.2 and ε_c=0.660%, for Figure 8, ρ_c=16.0 and ε_c=0.449%.

A summary of the results for the carbon/Kevlar simulations is shown in Table 8. The table contains the deterministic lay-up sequence of the fibers where just the key cluster that is repeated is given. Also, the table contains the percent of H-fibers in the hybrid, the estimator for the hybrid shape parameter ρ_c, the

estimator for the hybrid scale parameter ε_c, the estimated expected value for ultimate hybrid strain μ_c, and the coefficient of variation in ultimate hybrid strain c.v. Finally, the table contains the estimated expected value for ultimate strength M_c computed from the rule-of-mixtures.

6. Conclusion

A shear lag analysis has been utilized to calculate the stress concentration factors induced by broken fibers in hybrid composites with various volume ratios and various arrangements of fibers. The model we used for calculating the stress concentration factors contains only 15 fibers. Therefore, when more than half of the fibers were broken, the concentration factor increase on a surviving fiber directly adjacent to broken fibers is not as severe as compared with the work made by Fukuda et al.. The reason for this is the boundary effect. We must remember what we assume when our model is subjected to a tensile stress. The axial displacement of boundary is linear with axial distance, and this influences the fibers adjacent to two boundaries. An alternative would be to consider the fibers to be arranged in the form of a thin tube, in which case no boundary effect would be present. It is apparent that the shear lag analysis also can be used for calculating the concentration factor of the surviving fiber when there are some fibers broken in a hybrid composite with a thin tube arrangement. We can extend this approach to develop a chain of bundles probability model developed by Harlow et al. [23], and the hybrid effect could be studied in further detail.

According to the calculations here it is apparent that the surviving fiber between two cracks has a larger stress concentration

than fibers directly adjacent to only one crack even, with an equal number of broken fibers in the cracks. In this context, the introduction of low modulus fibers into a high modulus fiber composite is advantageous because the low modulus fibers act as crack arrestors. From the simulation, we find that when a low modulus fiber between two cracks breaks, then crack propagation and failure can be expected. However, the low modulus fiber can stop crack growth for small crack sizes. This can be seen from the increase in mean breaking strain for the hybrids compared to an all high modulus fiber composite, see Table 8. The 'hybrid effect' for strain have been shown to exist, because the simulations has shown that when hybrid composites contained higher ratio of L-fibers has higher mean breaking strain but it doesn't defer to the rule-of-mixture. Even in the worst cases of a very small percentage of L-fibers or of rather severe clumping of H-fibers, there was evidence of the 'hybrid effect'. There is also a positive effect for ultimate strength.

The chain-of-bundles probability model has been adapted to model interply hybrid composites consisting of various volume ratios in fiber arrangements. The hybrid structures studied were assumed to be constructed with a deterministically arranged regular pattern of H-fibers and L-fibers. The analysis was made by employing Monte Carlo simulation so that a variety of hybrid systems could be studied.

In order to check the accuracy and range of validity of the simulations, comparisons were made with some of the analytical results given in [19]. The simulations were reasonably close to the mathematically derived results for ultimate strain of hybrid. For example, the percent differences in the simulated medians and theoretical medians for ultimate strains ranged from 2.6% to 6.0%. Likewise, the percent differences in coefficient of variation ranged from 4.4% to 20.9%. The statistical behavior predicted by the simulations is characteristic of the limited experimental data available. The Weibull c.d.f. is a good choice to represent the hybrid breaking strain for laboratory size specimens. The coefficients of variation for the hybrid systems were typically in the 3-5% range, as expected from experiments. There is certainly a need for more statistically significant experiments to be conducted so that the statistical causes and effects can be described more accurately.

Table 1. Comparation for Concentration Factor with Fukuda et al..

Broken Fibers	R = 1		R = 3			
			Low Modulus		High modulus	
	Yang	Fukuda	Yang	Fukuda	Yang	Fukuda
1	1.331	1.343	1.771	1.774	1.131	---
2	1.650	1.600	2.027	2.171	1.405	1.400
3	1.875	1.789	2.478	2.495	1.511	1.571
4	2.195	2.048	2.657	2.771	1.709	1.724
5	2.347	2.210	2.974	3.075	1.791	1.875
6	2.670	2.371	3.098	3.335	1.946	2.021
7	2.751	2.524	3.345	3.514	1.991	2.127
8	3.033	2.710	3.445	3.714	2.089	2.229

Table 2. Concentration factor with extensional stiffness R_1=1.

H	L	H	L	H	L	H	L	H	L	H	L	H	L	H
1.002	1.004	1.008	1.014	1.027	1.065	1.331	*	1.331	1.065	1.027	1.014	1.008	1.004	1.002
1.001	1.003	1.005	1.008	1.014	1.027	1.065	1.331	*	1.331	1.065	1.026	1.013	1.007	1.003
1.005	1.011	1.019	1.033	1.061	1.137	1.592	*	*	1.592	1.136	1.060	1.031	1.017	1.008
1.003	1.007	1.012	1.021	1.038	1.085	1.383	*	1.708	*	1.382	1.083	1.035	1.017	1.007
1.005	1.011	1.020	1.037	1.084	1.383	*	1.708	*	1.383	1.084	1.037	1.020	1.011	1.005
1.013	1.028	1.051	1.095	1.206	1.810	*	*	*	1.810	1.206	1.095	1.051	1.028	1.013
1.008	1.018	1.032	1.054	1.097	1.207	1.811	*	*	*	1.808	1.203	1.091	1.046	1.025
1.018	1.044	1.105	1.440	*	2.005	*	*	1.635	1.154	1.070	1.039	1.023	1.013	1.006
1.009	1.020	1.037	1.069	1.153	1.635	*	*	2.007	*	1.443	1.108	1.049	1.025	1.011
1.018	1.039	1.071	1.129	1.271	1.998	*	*	*	*	1.995	1.267	1.124	1.063	1.027
1.017	1.039	1.078	1.171	1.685	*	*	2.332	*	*	1.685	1.171	1.078	1.039	1.017
1.028	1.070	1.166	1.681	*	*	2.332	*	*	1.687	1.174	1.081	1.044	1.024	1.011
1.010	1.021	1.038	1.067	1.136	1.505	*	2.256	*	*	*	1.838	1.210	1.089	1.036
1.021	1.050	1.099	1.217	1.844	*	*	*	2.257	*	1.504	1.135	1.064	1.034	1.015
1.035	1.080	1.154	1.325	2.159	*	*	*	*	*	2.159	1.325	1.154	1.080	1.035
1.057	1.138	1.313	2.148	*	*	*	*	*	2.162	1.330	1.162	1.090	1.050	1.023
1.040	1.098	1.227	1.282	*	*	*	2.604	*	*	1.738	1.193	1.090	1.046	1.020
1.088	1.249	1.999	*	*	*	*	2.466	*	1.562	1.162	1.083	1.048	1.027	1.013
1.033	1.081	1.187	1.733	*	*	2.604	*	*	*	1.889	1.234	1.108	1.055	1.024
1.019	1.042	1.079	1.160	1.562	*	2.473	*	*	*	*	2.018	1.269	1.117	1.048
1.068	1.163	1.363	2.290	*	*	*	*	*	*	2.302	1.377	1.182	1.095	1.042
1.093	1.262	2.036	*	*	*	*	2.834	*	*	1.788	1.214	1.102	1.053	1.023
1.038	1.092	1.207	1.783	*	*	2.838	*	*	*	*	2.056	1.283	1.125	1.051
1.107	1.297	2.151	*	*	*	*	*	2.657	*	1.614	1.184	1.094	1.051	1.023
1.027	1.061	1.118	1.252	1.934	*	*	*	2.888	*	*	*	1.911	1.226	1.080
1.059	1.143	1.323	2.175	*	*	*	*	*	2.660	*	1.610	1.178	1.083	1.035
1.044	1.107	1.244	1.928	*	*	*	2.893	*	*	*	1.968	1.244	1.107	1.044
1.048	1.109	1.207	1.423	2.420	*	*	*	*	*	*	*	2.382	1.374	1.137
1.086	1.241	1.953	*	*	*	3.137	*	*	*	*	2.095	1.298	1.132	1.054

1.042	1.102	1.226	1.829	*	*	3.039	*	*	*	*	*	2.183	1.309	1.111
1.077	1.186	1.408	2.415	*	*	*	*	*	*	*	2.415	1.408	1.186	1.077
1.048	1.116	1.261	1.971	*	*	*	3.137	*	*	*	*	2.074	1.275	1.098
1.075	1.208	1.814	*	*	3.037	*	*	*	*	*	2.208	1.335	1.150	1.062
1.086	1.206	1.448	2.522	*	*	*	*	*	*	*	*	2.488	1.410	1.151
1.104	1.288	2.110	*	*	*	*	3.392	*	*	*	*	2.110	1.288	1.104
1.082	1.223	1.854	*	*	3.212	*	*	*	*	*	*	2.312	1.351	1.128
1.046	1.111	1.242	1.869	*	*	3.205	*	*	*	*	*	*	2.245	1.275
1.228	2.059	*	*	*	*	3.380	*	*	*	*	2.130	1.312	1.139	1.058

Table 3. Concentration factor with extensional stiffness R_1=2.

H	L	H	L	H	L	H	L	H	L	H	L	H	L	H
1.001	1.002	1.004	1.008	1.014	1.040	1.186	*	1.186	1.040	1.014	1.008	1.004	1.002	1.001
1.002	1.005	1.008	1.014	1.022	1.045	1.097	1.570	*	1.570	1.096	1.044	1.021	1.011	1.005
1.005	1.011	1.018	1.032	1.055	1.130	1.454	*	*	1.827	1.153	1.071	1.035	1.019	1.008
1.002	1.004	1.006	1.011	1.020	1.050	1.209	*	1.387	*	1.208	1.050	1.019	1.010	1.004
1.008	1.018	1.032	1.063	1.131	1.680	*	2.263	*	1.680	1.131	1.063	1.032	1.018	1.008
1.015	1.035	1.062	1.121	1.245	2.173	*	*	*	2.173	1.245	1.121	1.061	1.035	1.015
1.007	1.016	1.027	1.047	1.079	1.181	1.592	*	*	*	1.590	1.177	1.074	1.039	1.016
1.025	1.066	1.146	1.740	*	2.573	*	*	1.517	1.157	1.070	1.041	1.024	1.014	1.006
1.009	1.021	1.037	1.076	1.161	1.854	*	*	1.679	*	1.266	1.078	1.034	1.018	1.008
1.019	1.044	1.077	1.149	1.297	2.355	*	*	*	*	1.786	1.255	1.112	1.061	1.025
1.017	1.040	1.074	1.172	1.555	*	*	2.917	*	*	1.555	1.172	1.074	1.040	1.017
1.030	1.080	1.178	1.918	*	*	1.998	*	*	1.925	1.186	1.091	1.046	1.026	1.011
1.014	1.031	1.053	1.100	1.193	1.856	*	3.000	*	*	*	2.239	1.258	1.118	1.044
1.017	1.041	1.078	1.184	1.606	*	*	*	1.829	*	1.301	1.095	1.044	1.024	1.010
1.031	1.073	1.134	1.298	1.891	*	*	*	*	*	1.891	1.298	1.134	1.073	1.031
1.064	1.166	1.355	2.591	*	*	*	*	*	2.608	1.373	1.193	1.102	1.058	1.026
1.048	1.126	1.273	2.288	*	*	*	3.373	*	*	1.622	1.203	1.091	1.050	1.021
1.081	1.245	1.807	*	*	*	*	3.218	*	1.916	1.215	1.114	1.061	1.036	1.016
1.033	1.087	1.192	1.959	*	*	2.164	*	*	*	1.649	1.203	1.088	1.048	1.020
1.015	1.034	1.060	1.124	1.357	*	2.042	*	*	*	*	2.360	1.288	1.133	1.050
1.072	1.187	1.395	2.727	*	*	*	*	*	*	2.041	1.362	1.167	1.092	1.039
1.086	1.256	1.835	*	*	*	*	3.609	*	*	1.659	1.220	1.101	1.056	1.024
1.039	1.100	1.216	2.028	*	*	2.397	*	*	*	*	2.412	1.305	1.142	1.054
1.090	1.270	1.874	*	*	*	*	*	2.155	*	1.388	1.141	1.070	1.040	1.018
1.022	1.051	1.095	1.215	1.674	*	*	*	2.333	*	*	*	1.656	1.193	1.063
1.068	1.176	1.373	2.650	*	*	*	*	*	3.535	*	2.000	1.238	1.116	1.046
1.054	1.140	1.299	2.370	*	*	*	3.869	*	*	*	2.370	1.299	1.140	1.054
1.044	1.102	1.185	1.396	2.122	*	*	*	*	*	*	*	2.085	1.350	1.120
1.070	1.210	1.697	*	*	*	2.576	*	*	*	*	2.444	1.315	1.147	1.056

1.042	1.108	1.229	2.066	*	*	2.521	*	*	*	*	*	1.905	1.282	1.095
1.085	1.217	1.453	2.919	*	*	*	*	*	*	*	2.919	1.453	1.217	1.085
1.057	1.148	1.314	2.415	*	*	*	4.126	*	*	*	*	1.883	1.276	1.093
1.076	1.219	1.695	*	*	3.943	*	*	*	*	*	2.685	1.384	1.182	1.070
1.092	1.234	1.485	3.022	*	*	*	*	*	*	*	*	2.196	1.394	1.137
1.097	1.287	1.909	*	*	*	*	4.392	*	*	*	*	1.909	1.287	1.097
1.081	1.232	1.725	*	*	4.123	*	*	*	*	*	*	2.061	1.342	1.117
1.047	1.119	1.249	2.120	*	*	2.687	*	*	*	*	*	*	2.662	1.297
1.243	2.408	*	*	*	*	2.814	*	*	*	*	2.493	1.331	1.156	1.060

Table 4. Concentration factor with extensional stiffness R_1=3.

H	L	H	L	H	L	H	L	H	L	H	L	H	L	H
1.001	1.002	1.003	1.005	1.010	1.030	1.131	•	1.131	1.030	1.010	1.005	1.003	1.002	1.001
1.003	1.006	1.010	1.017	1.027	1.057	1.117	1.771	•	1.771	1.117	1.055	1.025	1.014	1.006
1.005	1.011	1.018	1.032	1.053	1.130	1.405	•	•	2.027	1.165	1.080	1.037	1.021	1.009
1.001	1.002	1.004	1.007	1.013	1.036	1.144	•	1.269	•	1.144	1.035	1.012	1.006	1.003
1.010	1.023	1.040	1.082	1.163	1.938	•	2.747	•	1.938	1.163	1.082	1.040	1.023	1.010
1.016	1.040	1.068	1.139	1.273	2.478	•	•	•	2.478	1.273	1.139	1.068	1.039	1.016
1.007	1.015	1.025	1.044	1.072	1.171	1.511	•	•	•	1.509	1.168	1.068	1.040	1.015
1.030	1.082	1.175	1.999	•	3.070	•	•	1.481	1.175	1.072	1.044	1.025	1.015	1.007
1.009	1.022	1.039	1.084	1.171	2.048	•	•	1.561	•	1.201	1.065	1.028	1.016	1.007
1.020	1.047	1.081	1.164	1.317	2.657	•	•	•	•	1.709	1.254	1.108	1.060	1.025
1.017	1.042	1.075	1.178	1.513	•	•	3.429	•	•	1.513	1.178	1.075	1.042	1.017
1.031	1.088	1.189	2.125	•	•	1.880	•	•	2.133	1.198	1.100	1.048	1.028	1.012
1.016	1.037	1.063	1.124	1.232	2.161	•	3.652	•	•	•	2.583	1.292	1.139	1.050
1.015	1.038	1.070	1.173	1.518	•	•	•	1.673	•	1.226	1.079	1.036	1.020	1.009
1.029	1.071	1.126	1.290	1.791	•	•	•	•	•	1.791	1.290	1.126	1.071	1.029
1.069	1.186	1.385	2.964	•	•	•	•	•	2.984	1.405	1.215	1.109	1.064	1.027
1.053	1.146	1.306	2.634	•	•	•	4.047	•	•	1.589	1.215	1.095	1.054	1.022
1.080	1.250	1.742	•	•	•	•	3.878	•	2.224	1.253	1.137	1.071	1.042	1.018
1.034	1.094	1.201	2.162	•	•	2.005	•	•	•	1.560	1.193	1.081	1.045	1.018
1.014	1.031	1.053	1.110	1.282	•	1.887	•	•	•	•	2.655	1.306	1.145	1.053
1.076	1.205	1.420	3.098	•	•	•	•	•	•	1.946	1.360	1.161	1.091	1.038
1.084	1.260	1.766	•	•	•	•	4.289	•	•	1.621	1.230	1.103	1.059	1.025
1.040	1.108	1.227	2.244	•	•	2.240	•	•	•	•	2.718	1.324	1.155	1.057
1.084	1.261	1.772	•	•	•	•	•	1.973	•	1.305	1.123	1.061	1.036	1.016
1.020	1.048	1.086	1.202	1.578	•	•	•	2.132	•	•	•	1.563	1.182	1.057
1.074	1.199	1.410	3.053	•	•	•	•	•	4.304	•	2.340	1.281	1.140	1.054
1.061	1.164	1.339	2.750	•	•	•	4.730	•	•	•	2.750	1.339	1.164	1.061
1.042	1.100	1.176	1.389	2.008	•	•	•	•	•	•	•	1.974	1.344	1.114
1.064	1.200	1.603	•	•	•	2.374	•	•	•	•	2.746	1.332	1.159	1.058

1.043	1.115	1.238	2.279	*	*	2.334	*	*	*	*	*	1.802	1.274	1.089
1.090	1.240	1.486	3.345	*	*	*	*	*	*	*	3.345	1.486	1.240	1.090
1.064	1.172	1.353	2.798	*	*	*	4.997	*	*	*	*	1.820	1.284	1.093
1.078	1.232	1.663	*	*	4.738	*	*	*	*	*	3.091	1.420	1.205	1.077
1.096	1.255	1.514	3.445	*	*	*	*	*	*	*	*	2.089	1.393	1.132
1.097	1.293	1.842	*	*	*	*	5.273	*	*	*	*	1.842	1.293	1.097
1.083	1.244	1.689	*	*	4.921	*	*	*	*	*	*	1.972	1.344	1.114
1.048	1.127	1.259	2.344	*	*	2.502	*	*	*	*	*	*	3.018	1.316
1.258	2.709	*	*	*	*	2.613	*	*	*	*	2.806	1.350	1.169	1.063

Table 5. Ineffective length with extensional stiffness R_1=1.

H	L	H	L	H	L	H	L	H	L	H	L	H	L	H
0.000	0.000	0.000	0.000	0.000	0.000	0.000	1.568	0.000	0.000	0.000	0.000	0.000	0.000	0.000
0.000	0.000	0.000	0.000	0.000	0.000	0.000	0.000	1.568	0.000	0.000	0.000	0.000	0.000	0.000
0.000	0.000	0.000	0.000	0.000	0.000	0.000	2.345	2.345	0.000	0.000	0.000	0.000	0.000	0.000
0.000	0.000	0.000	0.000	0.000	0.000	0.000	1.677	0.000	1.676	0.000	0.000	0.000	0.000	0.000
0.000	0.000	0.000	0.000	0.000	1.677	0.000	1.677	0.000	0.000	0.000	0.000	0.000	0.000	0.000
0.000	0.000	0.000	0.000	0.000	2.917	3.500	2.917	0.000	0.000	0.000	0.000	0.000	0.000	0.000
0.000	0.000	0.000	0.000	0.000	0.000	2.916	3.498	2.914	0.000	0.000	0.000	0.000	0.000	0.000
0.000	0.000	0.000	0.000	1.792	0.000	2.492	2.442	0.000	0.000	0.000	0.000	0.000	0.000	0.000
0.000	0.000	0.000	0.000	0.000	0.000	2.442	2.494	0.000	1.795	0.000	0.000	0.000	0.000	0.000
0.000	0.000	0.000	0.000	0.000	0.000	3.380	4.346	4.344	3.378	0.000	0.000	0.000	0.000	0.000
0.000	0.000	0.000	0.000	0.000	2.554	2.654	0.000	2.654	2.554	0.000	0.000	0.000	0.000	0.000
0.000	0.000	0.000	0.000	2.549	2.650	0.000	2.654	2.555	0.000	0.000	0.000	0.000	0.000	0.000
0.000	0.000	0.000	0.000	0.000	0.000	1.909	0.000	3.086	3.628	2.990	0.000	0.000	0.000	0.000
0.000	0.000	0.000	0.000	0.000	2.998	3.635	3.090	0.000	1.909	0.000	0.000	0.000	0.000	0.000
0.000	0.000	0.000	0.000	0.000	3.769	5.027	5.387	5.027	3.769	0.000	0.000	0.000	0.000	0.000
0.000	0.000	0.000	0.000	3.757	5.015	5.379	5.023	3.769	0.000	0.000	0.000	0.000	0.000	0.000
0.000	0.000	0.000	0.000	3.090	3.785	3.274	0.000	2.808	2.665	0.000	0.000	0.000	0.000	0.000
0.000	0.000	0.000	3.415	4.428	4.479	3.556	0.000	2.011	0.000	0.000	0.000	0.000	0.000	0.000
0.000	0.000	0.000	0.000	2.660	2.805	0.000	3.278	3.792	3.097	0.000	0.000	0.000	0.000	0.000
0.000	0.000	0.000	0.000	0.000	2.013	0.000	3.570	4.500	4.453	3.439	0.000	0.000	0.000	0.000
0.000	0.000	0.000	0.000	4.092	5.588	6.214	6.218	5.597	4.104	0.000	0.000	0.000	0.000	0.000
0.000	0.000	0.000	3.501	4.567	4.664	3.764	0.000	2.948	2.768	0.000	0.000	0.000	0.000	0.000
0.000	0.000	0.000	0.000	2.765	2.947	0.000	3.777	4.685	4.493	3.526	0.000	0.000	0.000	0.000
0.000	0.000	0.000	3.788	5.084	5.491	5.183	3.966	0.000	2.106	0.000	0.000	0.000	0.000	0.000
0.000	0.000	0.000	0.000	0.000	3.196	3.944	3.454	0.000	3.441	3.922	3.171	0.000	0.000	0.000
0.000	0.000	0.000	0.000	3.819	5.117	5.519	5.203	3.977	0.000	2.104	0.000	0.000	0.000	0.000
0.000	0.000	0.000	0.000	3.190	3.940	3.454	0.000	3.454	3.940	3.190	0.000	0.000	0.000	0.000
0.000	0.000	0.000	0.000	0.000	4.390	6.076	6.898	7.144	6.875	6.034	4.342	0.000	0.000	0.000
0.000	0.000	0.000	3.264	4.066	3.606	0.000	3.970	4.863	4.731	3.612	0.000	0.000	0.000	0.000

0.000	0.000	0.000	0.000	2.860	3.074	0.000	4.188	5.387	5.656	5.206	3.862	0.000	0.000	0.000
0.000	0.000	0.000	0.000	4.382	6.076	6.909	7.167	6.909	6.076	4.382	0.000	0.000	0.000	0.000
0.000	0.000	0.000	0.000	3.283	4.083	3.615	0.000	3.961	4.845	4.706	3.588	0.000	0.000	0.000
0.000	0.000	0.000	2.845	3.064	0.000	4.195	5.404	5.682	5.238	3.893	0.000	0.000	0.000	0.000
0.000	0.000	0.000	0.000	4.631	6.489	7.489	7.940	7.931	7.464	6.452	4.592	0.000	0.000	0.000
0.000	0.000	0.000	3.669	4.837	5.012	4.138	0.000	4.138	5.012	4.847	3.669	0.000	0.000	0.000
0.000	0.000	0.000	2.930	3.177	0.000	4.548	5.991	6.529	6.444	5.741	4.172	0.000	0.000	0.000
0.000	0.000	0.000	0.000	2.941	3.183	0.000	4.522	5.945	6.465	6.364	5.651	4.090	0.000	0.000
0.000	0.000	3.610	4.776	4.963	4.108	0.000	4.138	5.022	4.855	3.691	0.000	0.000	0.000	0.000

Table 6. Ineffective length with extensional stiffness R_1=2.

H	L	H	L	H	L	H	L	H	L	H	L	H	L	H
0.000	0.000	0.000	0.000	0.000	0.000	0.000	1.069	0.000	0.000	0.000	0.000	0.000	0.000	0.000
0.000	0.000	0.000	0.000	0.000	0.000	0.000	0.000	1.641	0.000	0.000	0.000	0.000	0.000	0.000
0.000	0.000	0.000	0.000	0.000	0.000	0.000	1.877	2.177	0.000	0.000	0.000	0.000	0.000	0.000
0.000	0.000	0.000	0.000	0.000	0.000	0.000	1.114	0.000	1.113	0.000	0.000	0.000	0.000	0.000
0.000	0.000	0.000	0.000	0.000	0.000	1.817	0.000	1.817	0.000	0.000	0.000	0.000	0.000	0.000
0.000	0.000	0.000	0.000	0.000	0.000	2.815	3.160	2.815	0.000	0.000	0.000	0.000	0.000	0.000
0.000	0.000	0.000	0.000	0.000	0.000	0.000	2.244	2.921	2.243	0.000	0.000	0.000	0.000	0.000
0.000	0.000	0.000	0.000	1.913	0.000	2.400	2.015	0.000	0.000	0.000	0.000	0.000	0.000	0.000
0.000	0.000	0.000	0.000	0.000	0.000	2.222	1.943	0.000	1.211	0.000	0.000	0.000	0.000	0.000
0.000	0.000	0.000	0.000	0.000	0.000	3.138	3.751	3.789	2.717	0.000	0.000	0.000	0.000	0.000
0.000	0.000	0.000	0.000	0.000	2.098	2.531	0.000	2.531	2.098	0.000	0.000	0.000	0.000	0.000
0.000	0.000	0.000	0.000	2.329	2.083	0.000	2.087	2.334	0.000	0.000	0.000	0.000	0.000	0.000
0.000	0.000	0.000	0.000	0.000	0.000	2.079	0.000	3.082	3.361	2.935	0.000	0.000	0.000	0.000
0.000	0.000	0.000	0.000	0.000	2.278	2.980	2.319	0.000	1.267	0.000	0.000	0.000	0.000	0.000
0.000	0.000	0.000	0.000	0.000	2.965	4.231	4.451	4.231	2.965	0.000	0.000	0.000	0.000	0.000
0.000	0.000	0.000	0.000	3.562	4.489	2.891	4.497	3.575	0.000	0.000	0.000	0.000	0.000	0.000
0.000	0.000	0.000	0.000	3.016	3.486	3.238	0.000	2.735	2.233	0.000	0.000	0.000	0.000	0.000
0.000	0.000	0.000	2.794	3.935	3.971	3.421	0.000	2.166	0.000	0.000	0.000	0.000	0.000	0.000
0.000	0.000	0.000	0.000	2.394	2.166	0.000	2.481	3.125	2.367	0.000	0.000	0.000	0.000	0.000
0.000	0.000	0.000	0.000	0.000	1.352	0.000	2.799	3.854	3.793	3.157	0.000	0.000	0.000	0.000
0.000	0.000	0.000	0.000	3.796	4.882	5.456	5.326	4.822	3.305	0.000	0.000	0.000	0.000	0.000
0.000	0.000	0.000	2.867	4.040	4.113	3.590	0.000	2.846	2.307	0.000	0.000	0.000	0.000	0.000
0.000	0.000	0.000	0.000	2.500	2.293	0.000	2.982	4.029	3.928	3.244	0.000	0.000	0.000	0.000
0.000	0.000	0.000	2.961	4.241	4.485	4.291	3.045	0.000	1.399	0.000	0.000	0.000	0.000	0.000
0.000	0.000	0.000	0.000	0.000	2.420	3.209	2.572	0.000	2.564	3.193	2.404	0.000	0.000	0.000
0.000	0.000	0.000	0.000	3.660	4.647	5.106	4.773	3.901	0.000	2.294	0.000	0.000	0.000	0.000
0.000	0.000	0.000	0.000	3.151	3.689	3.484	0.000	3.484	3.689	3.151	0.000	0.000	0.000	0.000
0.000	0.000	0.000	0.000	0.000	3.485	5.133	5.776	6.068	5.758	5.100	3.452	0.000	0.000	0.000
0.000	0.000	0.000	2.489	3.329	2.708	0.000	3.084	4.130	4.007	3.296	0.000	0.000	0.000	0.000

0.000	0.000	0.000	0.000	2.559	2.363	0.000	3.238	4.480	4.638	4.355	3.028	0.000	0.000	0.000
0.000	0.000	0.000	0.000	4.123	5.416	6.204	6.352	6.204	5.416	4.123	0.000	0.000	0.000	0.000
0.000	0.000	0.000	0.000	3.225	3.800	3.617	0.000	3.854	4.344	4.216	2.961	0.000	0.000	0.000
0.000	0.000	0.000	2.403	3.001	0.000	4.082	4.933	5.234	4.741	3.720	0.000	0.000	0.000	0.000
0.000	0.000	0.000	0.000	4.297	5.699	6.596	6.878	6.893	6.380	5.537	3.705	0.000	0.000	0.000
0.000	0.000	0.000	3.019	4.313	4.471	3.997	0.000	3.997	4.471	4.313	3.019	0.000	0.000	0.000
0.000	0.000	0.000	2.464	3.091	0.000	4.336	5.343	5.816	5.589	4.994	3.393	0.000	0.000	0.000
0.000	0.000	0.000	0.000	2.642	2.460	0.000	3.570	5.050	5.480	5.537	4.900	3.765	0.000	0.000
0.000	0.000	3.296	4.054	4.228	3.205	0.000	3.233	4.283	4.127	3.376	0.000	0.000	0.000	0.000

Table 7. Ineffective length with extensional stiffness R_1=3.

H	L	H	L	H	L	H	L	H	L	H	L	H	L	H
0.000	0.000	0.000	0.000	0.000	0.000	0.000	0.858	0.000	0.000	0.000	0.000	0.000	0.000	0.000
0.000	0.000	0.000	0.000	0.000	0.000	0.000	0.000	1.690	0.000	0.000	0.000	0.000	0.000	0.000
0.000	0.000	0.000	0.000	0.000	0.000	0.000	1.690	2.124	0.000	0.000	0.000	0.000	0.000	0.000
0.000	0.000	0.000	0.000	0.000	0.000	0.000	0.884	0.000	0.884	0.000	0.000	0.000	0.000	0.000
0.000	0.000	0.000	0.000	0.000	0.000	1.914	0.000	1.914	0.000	0.000	0.000	0.000	0.000	0.000
0.000	0.000	0.000	0.000	0.000	0.000	2.804	3.055	2.804	0.000	0.000	0.000	0.000	0.000	0.000
0.000	0.000	0.000	0.000	0.000	0.000	0.000	1.976	2.705	1.975	0.000	0.000	0.000	0.000	0.000
0.000	0.000	0.000	0.000	2.001	0.000	2.400	1.855	0.000	0.000	0.000	0.000	0.000	0.000	0.000
0.000	0.000	0.000	0.000	0.000	0.000	2.153	1.730	0.000	0.971	0.000	0.000	0.000	0.000	0.000
0.000	0.000	0.000	0.000	0.000	0.000	3.067	3.538	3.590	2.456	0.000	0.000	0.000	0.000	0.000
0.000	0.000	0.000	0.000	0.000	1.926	2.516	0.000	2.516	1.926	0.000	0.000	0.000	0.000	0.000
0.000	0.000	0.000	0.000	2.259	1.862	0.000	1.865	2.266	0.000	0.000	0.000	0.000	0.000	0.000
0.000	0.000	0.000	0.000	0.000	0.000	2.202	0.000	3.143	3.308	2.959	0.000	0.000	0.000	0.000
0.000	0.000	0.000	0.000	0.000	1.996	2.741	2.020	0.000	1.008	0.000	0.000	0.000	0.000	0.000
0.000	0.000	0.000	0.000	0.000	2.647	3.935	4.097	3.935	2.647	0.000	0.000	0.000	0.000	0.000
0.000	0.000	0.000	0.000	3.520	4.318	4.736	4.326	3.535	0.000	0.000	0.000	0.000	0.000	0.000
0.000	0.000	0.000	0.000	3.031	3.419	3.284	0.000	2.756	2.077	0.000	0.000	0.000	0.000	0.000
0.000	0.000	0.000	2.557	3.777	3.816	3.426	0.000	2.281	0.000	0.000	0.000	0.000	0.000	0.000
0.000	0.000	0.000	0.000	2.309	1.919	0.000	2.171	2.881	2.081	0.000	0.000	0.000	0.000	0.000
0.000	0.000	0.000	0.000	0.000	1.083	0.000	2.503	3.626	3.558	3.073	0.000	0.000	0.000	0.000
0.000	0.000	0.000	0.000	3.711	4.634	5.188	5.000	4.541	2.990	0.000	0.000	0.000	0.000	0.000
0.000	0.000	0.000	2.609	3.868	3.940	3.577	0.000	2.853	2.139	0.000	0.000	0.000	0.000	0.000
0.000	0.000	0.000	0.000	2.416	2.039	0.000	2.675	3.798	3.692	3.161	0.000	0.000	0.000	0.000
0.000	0.000	0.000	2.637	3.931	4.109	3.965	2.692	0.000	1.114	0.000	0.000	0.000	0.000	0.000
0.000	0.000	0.000	0.000	0.000	2.117	2.941	2.233	0.000	2.226	2.928	2.105	0.000	0.000	0.000
0.000	0.000	0.000	0.000	3.645	4.515	5.005	4.671	3.946	0.000	2.433	0.000	0.000	0.000	0.000
0.000	0.000	0.000	0.000	3.191	3.656	3.577	0.000	3.577	3.656	3.191	0.000	0.000	0.000	0.000
0.000	0.000	0.000	0.000	0.000	3.129	4.783	5.355	5.670	5.339	4.754	3.101	0.000	0.000	0.000
0.000	0.000	0.000	2.186	3.061	2.360	0.000	3.746	3.872	3.750	3.200	0.000	0.000	0.000	0.000

0.000	0.000	0.000	0.000	2.461	2.089	0.000	2.871	4.149	4.259	4.042	2.702	0.000	0.000	0.000
0.000	0.000	0.000	0.000	4.060	5.197	5.969	6.073	5.969	5.197	4.060	0.000	0.000	0.000	0.000
0.000	0.000	0.000	0.000	3.257	3.754	3.696	0.000	3.888	4.206	4.069	2.726	0.000	0.000	0.000
0.000	0.000	0.000	2.247	3.033	0.000	4.110	4.812	5.117	4.598	3.698	0.000	0.000	0.000	0.000
0.000	0.000	0.000	0.000	4.202	5.424	6.281	6.495	6.518	5.980	5.202	3.357	0.000	0.000	0.000
0.000	0.000	0.000	2.775	4.152	4.315	4.015	0.000	4.015	4.315	4.152	2.775	0.000	0.000	0.000
0.000	0.000	0.000	2.297	3.112	0.000	4.320	5.148	5.587	5.294	4.734	3.092	0.000	0.000	0.000
0.000	0.000	0.000	0.000	2.546	2.180	0.000	3.204	4.730	5.124	5.246	4.636	3.668	0.000	0.000
0.000	0.000	3.200	3.797	3.968	2.858	0.000	2.886	4.023	3.870	3.282	0.000	0.000	0.000	0.000

Table 8. Simulated results for carbon/Kevlar hybrids.

Lay-up Sequence	Percent of H-fibers	ρ_c	ε_c (%)	μ_c (%)	c.v. (%)	Mc (GPa)
H	100	15.978	0.449	0.4349	7.39	0.991
2H:1L	67	24.711	0.521	0.5098	4.91	0.881
1H:1L	50	28.196	0.660	0.6474	4.33	0.851

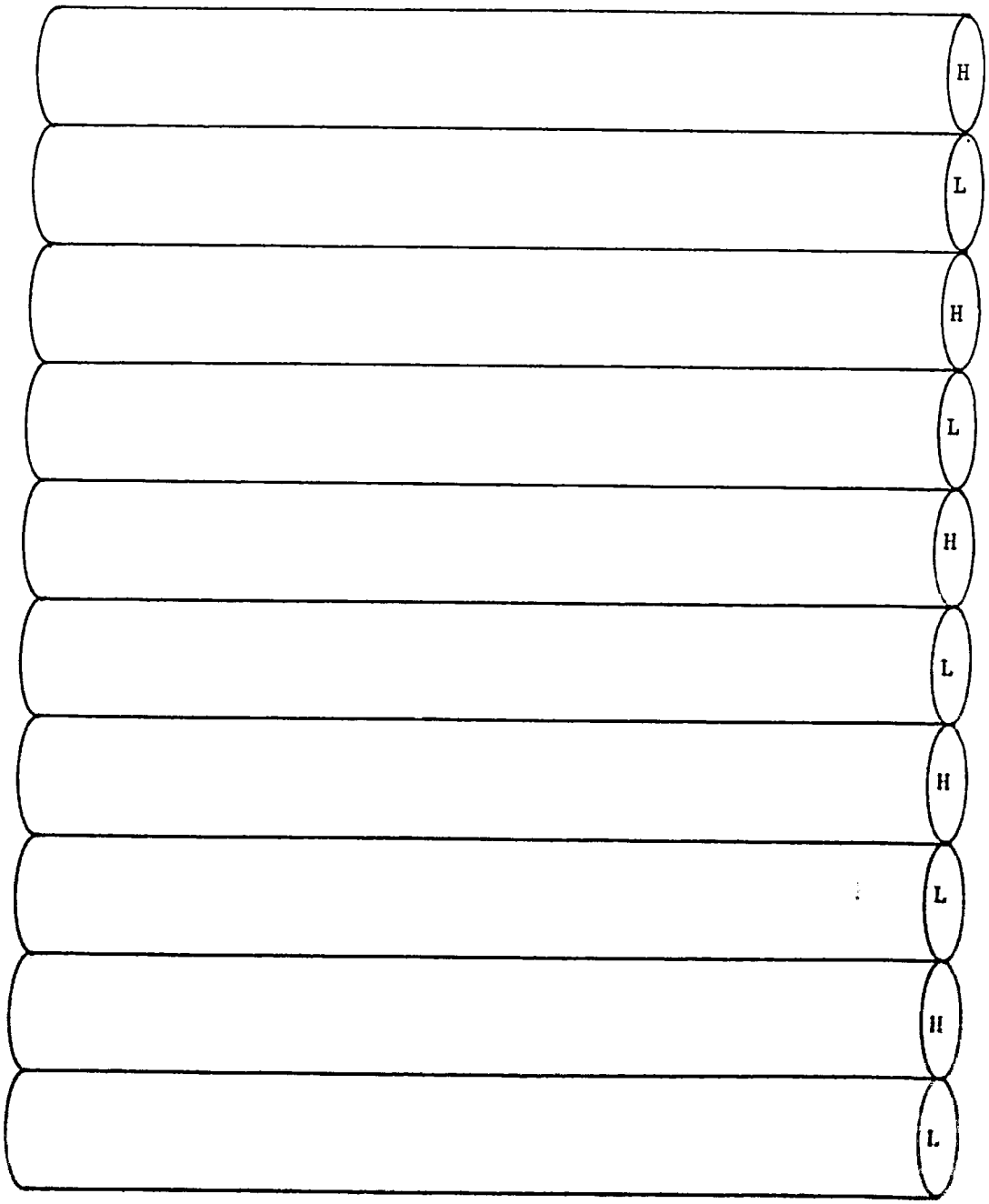

Figure 1. A schematic of planar hybrid composite tape with alternated H-fibers and L-fibers.

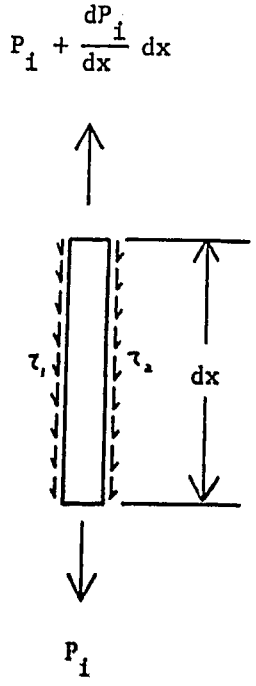

Figure 2. Equilibrium diagram of a single fiber.

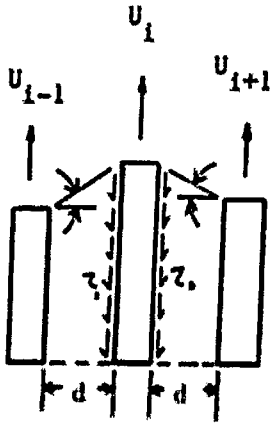

Figure 3. Model for tensile strength analysis of three composite fibers.

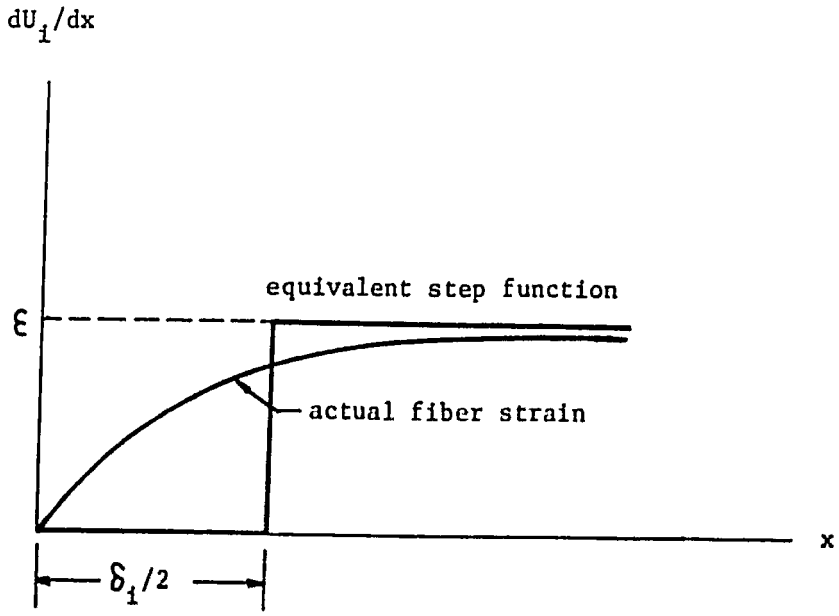

Figure 4. Definition of ineffective length.
(after Friedman [18])

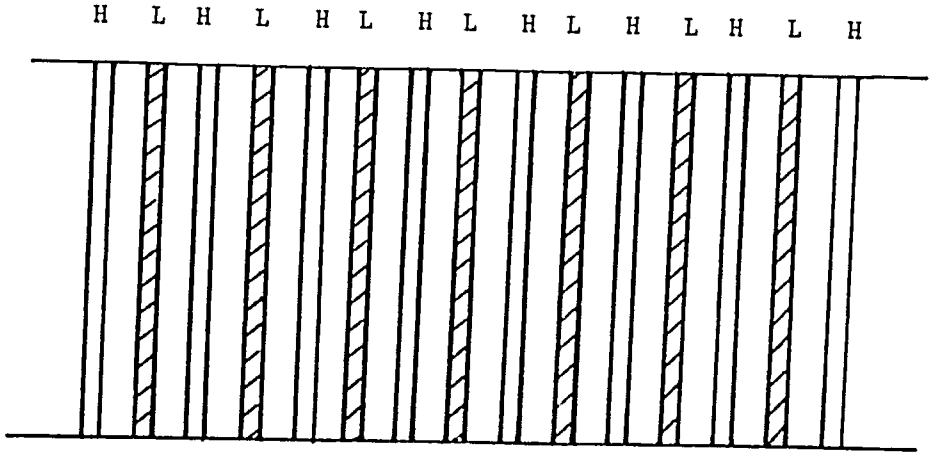

Figure 5. Model for stress concentration factor analysis of hybrid composite.

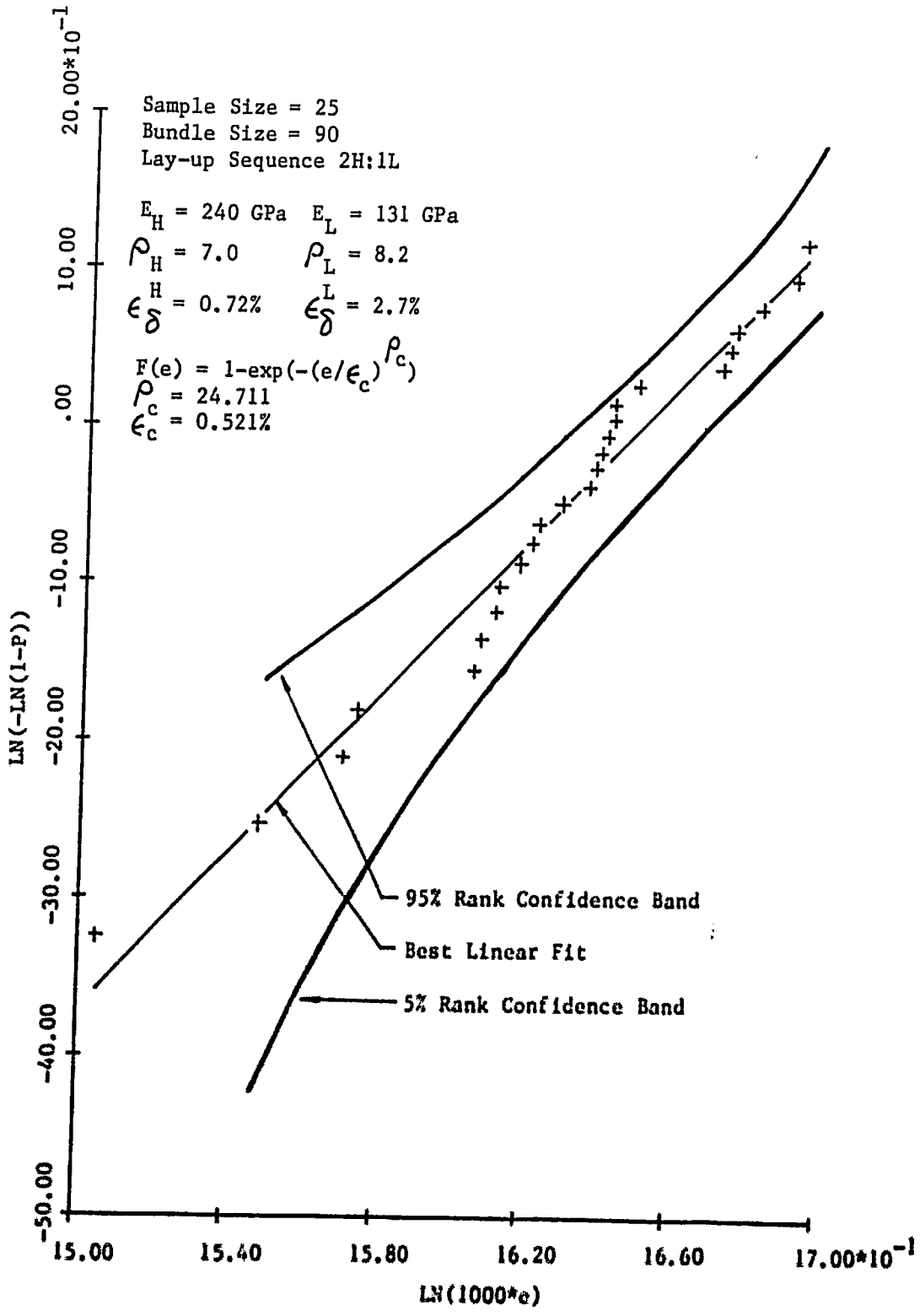

Figure 6. The simulated Weibull c.d.f. for breaking strain of a 2H:1L hybrid composite is shown.

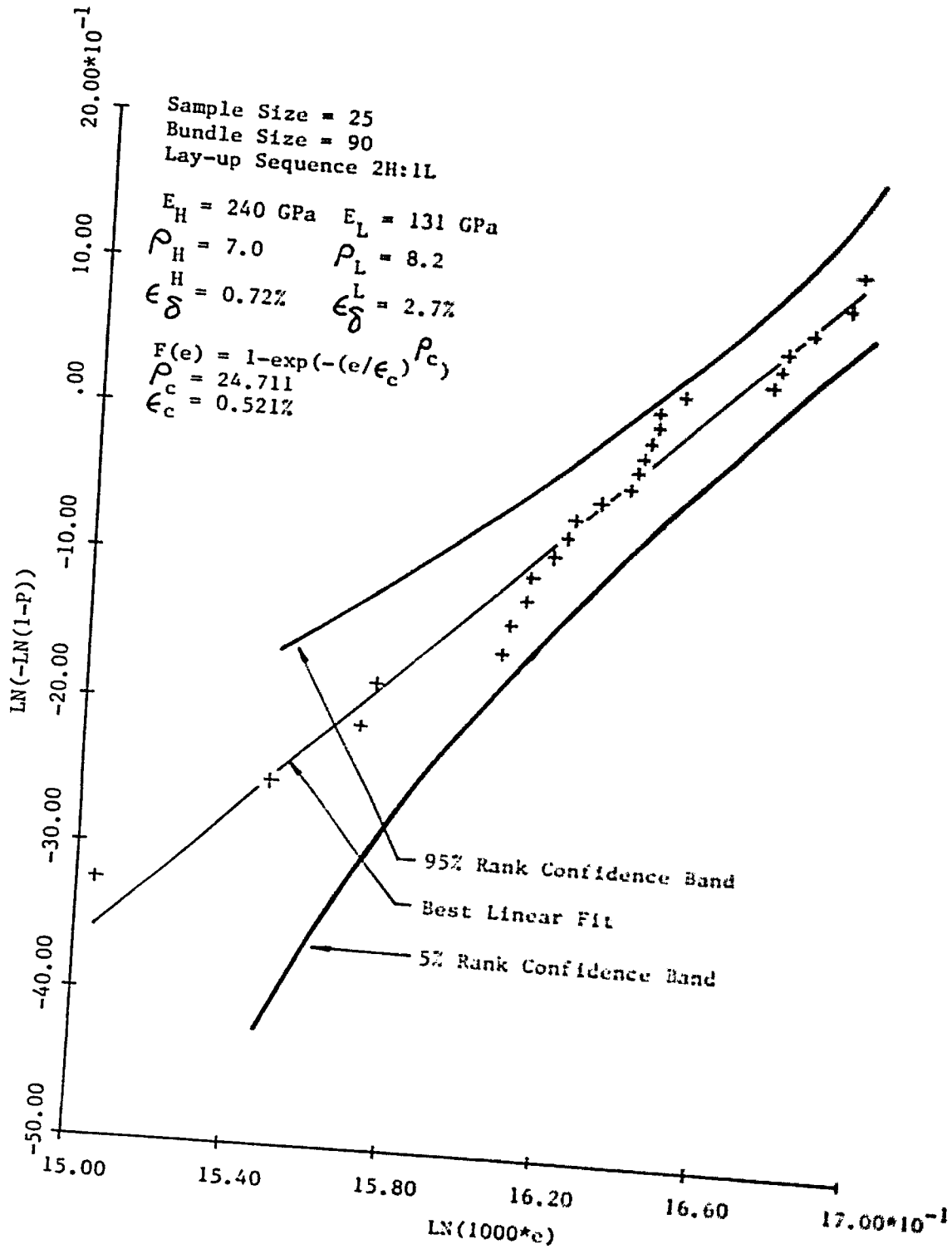

Figure 6. The simulated Weibull c.d.f. for breaking strain of a 2H:1L hybrid composite is shown.

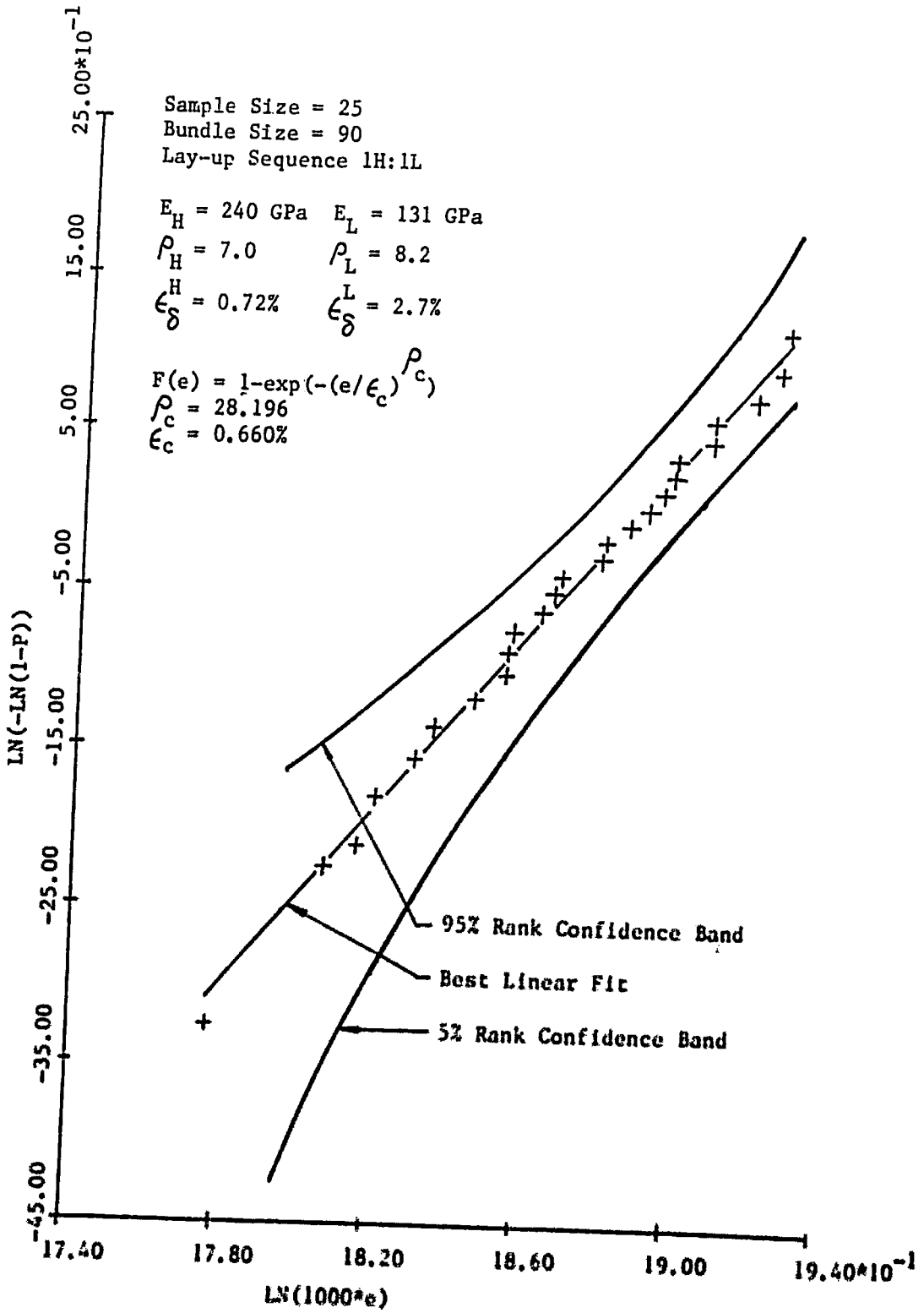

Figure 7. The simulated Weibull c.d.f. for breaking strain of a 1H:1L hybrid composite is shown.

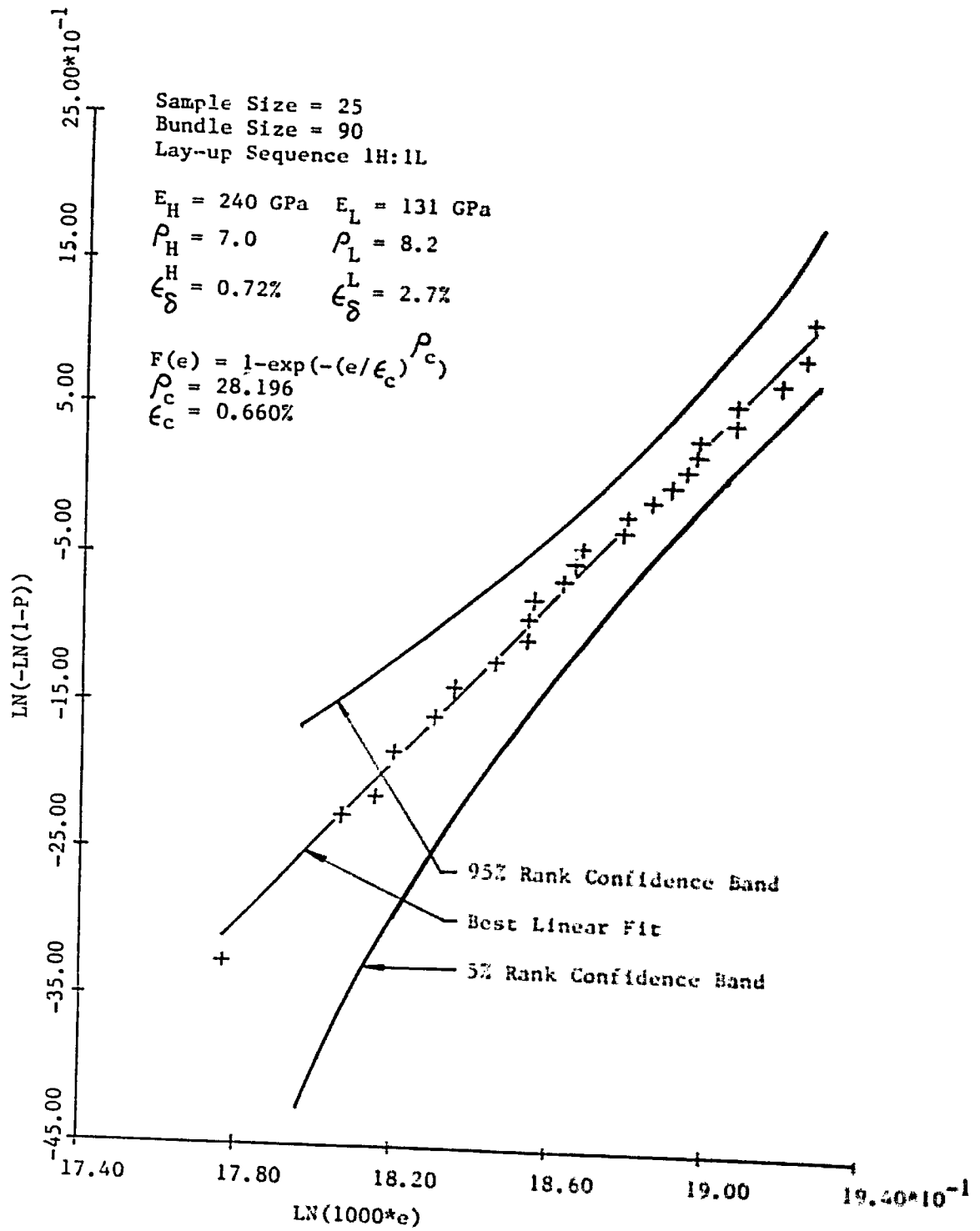

Figure 7. The simulated Weibull c.d.f. for breaking strain of a 1H:1L hybrid composite is shown.

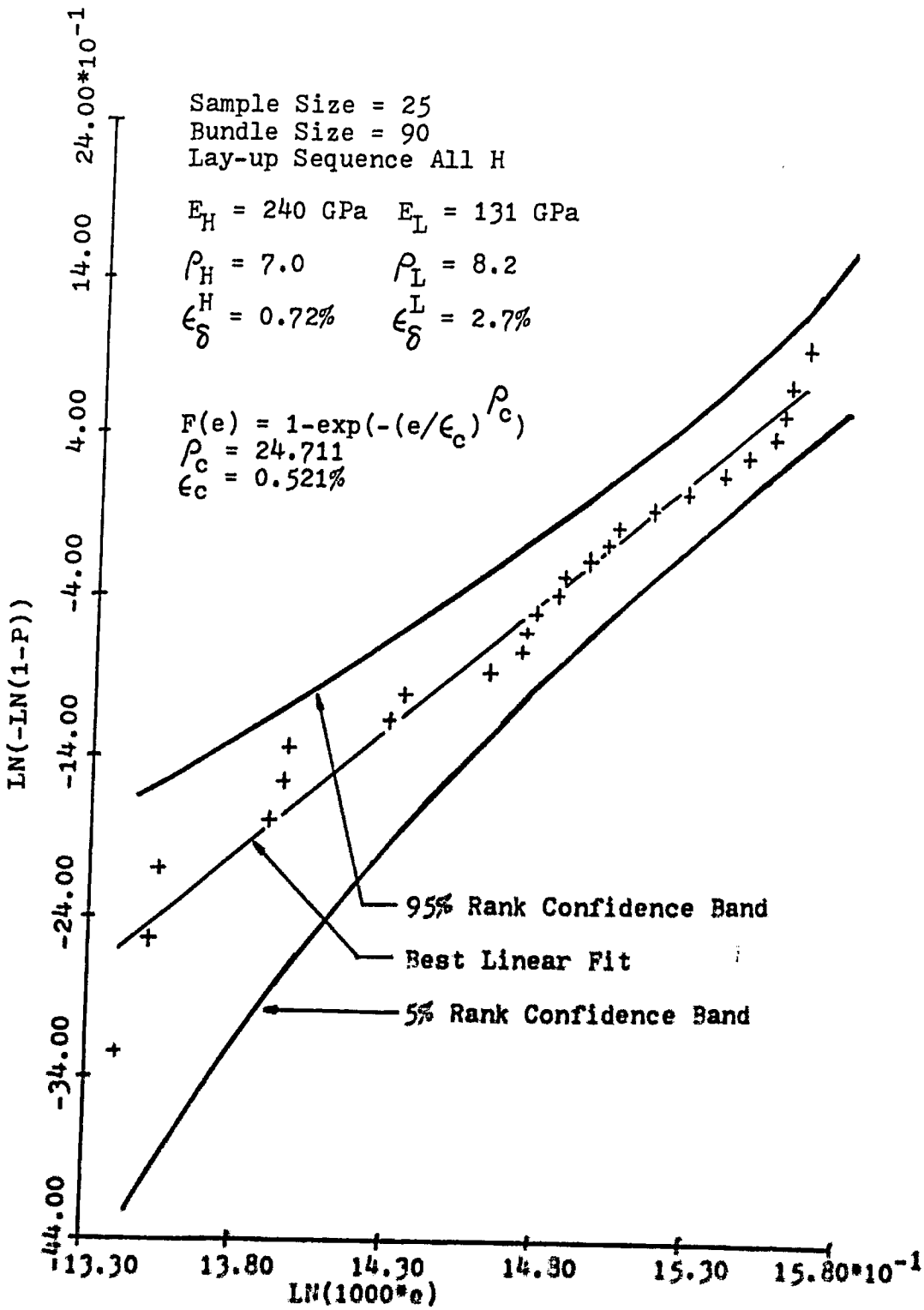

Figure 8. The simulated Weibull c.d.f. for breaking strain of all H composite is shown.

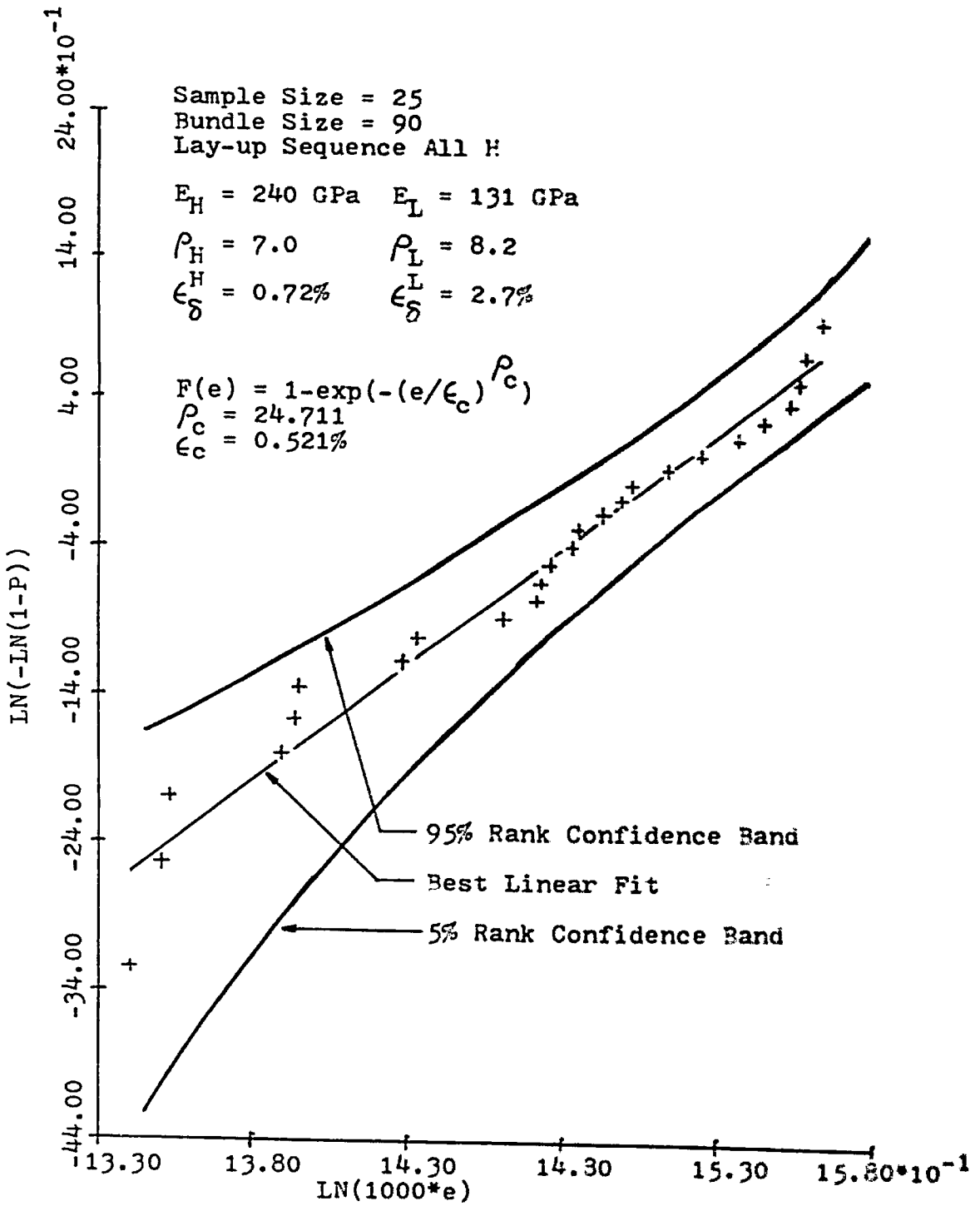

Figure 8. The simulated Weibull c.d.f. for breaking strain of all H composite is shown.

7. References

1. D. R. Lovell, 'Hybrid Laminates of Glass/Carbon fibers-1,' Reinforced Plastics, Vol. 22 (1978), P. 216.

2. D. R. Lovell, 'Hybrid Laminates of Glass/Carbon Fibers-2,' Reinforced Plastics, Vol. 22 (1978), p. 252.

3. L. N. Phillips, 'On the Usefulness of Glass Fiber-Carbon Hybrids,' Proc. 10th Inter. Reinforced Plastics Conf., Brighton, England (Nov. 1976), P. 207.

4. L. N. Phillips, 'Carbon Fiber Reinforced Plastics - The First Fifteen Years', Plastics and Rubber Inter., Vol. 3 (1978), p. 239.

5. M. G. Phillips, 'Composition Parameters for Hybrid Composite Materials', Composites, Vol. 12 (1981), p. 113.

6. D. Short and J. Summerscales, 'Hybrids - A Review, Part 1. Techniques, Design, and Construction', Composites, Vol. 10 (1979), p. 215.

7. D. Short and J. Summerscales, 'Hybrids - A Review, Part 2. Physical Properties', Composites, Vol. 11 (1980), p. 33.

8. J. Summerscales and D. Short, 'Carbon Fiber and Glass Fiber Hybrid Reinforced Plastics', Composites, Vol. 9 (1978), p. 157.

9. G. Marom, S. Fischer, F. R. Tuler, and H. D. Wagner, 'Hybrid Effects in Composites: Conditions for Positive or Negative Effects Versus Rule-of-Mixtures Behavior', J. Material Science, Vol. 13 (1978), p. 1419.

10. T. Hayashi, 'Proceedings of the Eight International Reinforced Plastics Conference', Brighton, (Oct. 1972), p. 22.

11. A. R. Bunsell and B. Harris, Composites, Vol. 5 (1974) p. 157.

12. C. C. Chamis, R. F. Lark, and J. H. Sinclair, 'Mechanical Property Characterization of Intraply Hybrid Composites', Test Methods and Design Allowables for Fibrous Composites, ASTM STP 734 (1981), p. 261.

13. C. Zweben, ',Tensile Strength of Hybrid Composites', J. Material Science, Vol. 12 (1977), p. 1325.

14. J. M. Hedgepeth, 'Stress Concentrations in Filamentary Structures', NASA TN D-882, (1961)

15. C. Zweben, 'An Approximate Method of Analysis for Notched Unidirectional Composites', Eng. Fracture Mechanics, Vol. 6, (1974), p. 1.

16. T. W. Chou and H. Fukuda, 'Stiffness and Strength of Hybrid Composites', Compostie Materials: Mechanics Mechanical Properties and Fabrication, K. Kawata and T. Akasaka, Japan Society for Composite Materials, (1981) p. 78-88.

17. H. Fukuda and T. W. Chou, 'Stress Concentration in a Hybrid Composite Sheet', J. Applied Mechanics, Vol. 50 (1983), p. 845.

18. E. Friedman, 'Society of the Plastics Industry', Washington, D. C. (Feb. 1967)

19. D. G. Harlow, 'Statistical Properties of Hybrid Composites I. Recursion Analysis', Proc. R. Soc. Lond. A, Vol. 389 (1983), P. 67.

20. S. L. Phoenix and E. M. Wu, 'Statistics for the Time-Dependent Failure of Kevlar-49/Epoxy Composites: Micromechanical Modeling and Data Interpretation', Proc. Inter. Union Theo. Appl. Mech. (Z. Hashin and C. T. Herakovich, ed.)

21. P. W. Manders and M. G. Bader, 'The Strength of Hybrid Glass/Carbon Fiber Composites, Part 2 A Statistical Model', J. Material Science, Vol. 16 (1981), P. 2246.

22. M. G. Bader and P. W. Manders, 'Failure Strain Enhancement in Carbon/Glass Fiber Hybrid Composites', Proc. 1978 I.C.C.M. (B. R. Noton, R. A. Signorelli, K. N. Street, and L. N. Phillips, ed.), A.I.M.E., New York (1978), P. 1147.

23. D. G. Harlow and S. L. Phoenix, 'The Chain-of-Bundles Probability Model for the Strength of Fibrous Materials, I. Analysis and Conjection' , J. Composite Material, Vol. 12 (1978), p. 195-214.

24. H. Fukuda and T.W. Chou, 'Monte Carlo Simulation of the Strength of Hybrid Composites', J. Composite Material, Vol. 16 (1982), p. 371.

VITA

Chwang-Liang Yang was born in Taipei, Taiwan, Republic of China on November 22, 1950. He graduated from National Taiwan University in June 1974 with a B.S. degree in Department of Agricultural Machinery and Engineering.

In January 1983, the author entered the Department of Mechanical Engineering and Mechanics at Lehigh University. Since then, he studied in the field of mechanics of composites material under Dr. T.J. Delph and Dr. D.G. Harlow.